

Received October 1, 2021, accepted October 19, 2021, date of publication October 27, 2021, date of current version November 8, 2021.

Digital Object Identifier 10.1109/ACCESS.2021.3123441

An Analytical Evaluation of the Shielding Effectiveness of Enclosures Containing Complex Apertures

AMÉLIE RABAT¹, PIERRE BONNET¹, KHALIL EL KHAMLI CHI DRISSI¹, (Senior Member, IEEE), AND SÉBASTIEN GIRARD¹

Université Clermont Auvergne, CNRS, Clermont Auvergne INP, Institut Pascal, F-63000 Clermont-Ferrand, France

Corresponding author: Amélie Rabat (amelie.rabat@gmail.com)

This work was supported in part by the Ministry of Higher Education and Scientific Research (MESR).

ABSTRACT Analytical methods are significantly useful tools for engineers in computational modeling. These methods provide fast simulations, while preserving physical meaning. In this paper, a full analytical formulation is developed based on the circuit approach, also known as Intermediate Level Circuit Model (ILCM), to evaluate the shielding effectiveness (SE) of metallic structures. The proposal focuses on rectangular enclosures containing apertures of complex geometrical shape, illuminated by an external plane wave. The enclosure is taken as a short-circuited waveguide. The aperture is treated as a transmission line with an intrinsic impedance that depends on the aperture polarizability, according to Bethe's theory of small holes. The formulation easily takes into account high-order resonant modes and different apertures, such as circular, elliptical, round-ended and cross-shaped apertures. The ILCM technique reveals good agreement with a numerical full-wave method for various configurations of enclosures, covering a large range of frequencies from 0.5 GHz to 2.5 GHz, thus offering perspectives for parametric and/or optimization SE studies.

INDEX TERMS Analytical formulation, circuit model, complex apertures, metallic enclosures, polarizability, shielding effectiveness.

I. INTRODUCTION

In solving electromagnetic (EM) field problems, numerical methods have become popular as a result of the development of accurate and efficient software associated with cost reductions and an increase in the speed of computational systems [1]–[4]. The lack of analytical solutions in the electromagnetic domain have led researchers and engineers to use numerical software extensively to solve many complex problems. Analytical methods are often confined to the simple validation of numerical approaches. However, they have significant competitive advantages. First of all, analytical methods provide a mathematical description of system behavior that allows for the understanding of the mechanism and physical effects by way of a model problem. This is done without heavy computational costs but is only applicable for problems that have been simplified. Secondly, when analytical methods do demonstrate sufficient accuracy, they can

be very useful for parametric or stochastic studies, as well as for system optimization. Indeed, such studies require a great number of efficient simulations involving the use of very fast and efficient tools, such as analytical approaches and models. Our paper focuses on the development of an analytical method in the EM domain. One particular topic of great interest for electrical and electronics engineers is the study of the interaction of an external electromagnetic field with an enclosure containing apertures, covering a large range of frequencies. On the one hand, conductive enclosure behavior is not a simple problem to be resolved analytically, except for canonical enclosures. On the other hand, apertures are mandatory for ventilation panels and output connections. Although there are sometimes unintentional apertures, their impact is always relevant. These various holes are responsible for significant EM disruptions in so far as they allow external radiation to penetrate inside the enclosure and, consequently, produce unintended EM coupling or interference. The EM field distribution inside the enclosure is not only dominated by the enclosure shape but also by the size, shape and

The associate editor coordinating the review of this manuscript and approving it for publication was Amedeo Andreotti¹.

location of the apertures. Electromagnetically, the shielding performance of the enclosure is evaluated by its shielding effectiveness (SE), corresponding to the ratio of fields in the absence and presence of the shield. Despite their simple geometric representation, neither the behavior, nor the SE of rectangular perforated shielding devices are simple to predict. Both the aperture and the design material may strongly affect the SE evaluation. Many numerical methods are available to efficiently calculate the SE of lossy enclosures containing apertures. Most of them are reported in [5, Ch.5, pp.87-143]. However, despite the significant improvements having been made in the development of numerical methods, the SE evaluation of enclosures containing holes, over a broad frequency range, remains computationally intensive. Thus, our paper focuses on the development of a fully analytical approach based on an Intermediate Level Circuit Model (ILCM) which is able to evaluate the rate of penetration of the electromagnetic fields inside a rectangular metallic enclosure with complex apertures.

According to Robinson *et al.* [6], who pioneered the ILCM analytical approach, the enclosure is considered as a short-circuited waveguide, modeled by an equivalent transmission line (TL). However, there are certain limitations to Robinson's method. Firstly, the method is developed only for one slot located at the center of the front panel. Secondly, only the waveguide dominant mode TE_{10} is considered. An incredible number of published studies rely on Robinson's proposal [7]. Unfortunately, their formulations contain the same restrictions regarding the range of frequencies and the aperture the shapes of the apertures. To overcome these limitations, Konefal *et al.* [8] and Yin and Du [9], proposed two different ILCM models. Both of them give a reliable prediction of SE at any observation point and simulate high order waveguide modes. Concerning the apertures, Konefal's model can handle an off-centered slot by introducing the radiation resistance of the slot and Yin's model can simulate many electrically small apertures of different, canonical shapes, by introducing an aperture coefficient C_a , in terms of aperture position.

Regrettably, all of these reported models can only cope with canonical aperture shapes, such as rectangle, square or circle. In fact, circular apertures are usually treated as square ones with equivalent surfaces. Obviously, this approach could only produce discrepancies in complex configurations. The formulation presented in this paper strives to overcome these aforementioned restrictions and to deal effectively with complex aperture shapes as well. In fact, elliptical apertures are useful in order to represent various shapes of regular apertures (such as non-symmetrical apertures), since the aperture surfaces and eccentricity will be equivalent. A few years ago, HongYi *et al.* [10] developed a novel approach to evaluate the SE of rectangular enclosures containing elliptical apertures and horizontal curved edge apertures. The aperture is modeled by many short, coplanar strip transmission lines connected in series in order to represent, as faithfully as possible, the realistic, horizontal curves of certain apertures. However,

even though Hong Yi *et al.* improved Robinson's model, their formulation still presents the same extreme limitations with respect to aperture position (centered) and waveguide excitation (dominant mode only). Another significant work has been reported by Solin [11]. He developed a fully analytical approach based on Bethe's theory for aperture coupling and Collin's perturbation method for wall losses [12], leading to a rigorous mathematical description of the problem of realistic enclosures. Also, the technique developed by Solin takes high order resonant modes of the enclosure into account. Despite its efficiency, the formulation is complex and focuses on a single, centered, circular aperture. The formulation could be applied to aperture shapes other than a circle, but the demonstration would be too tedious to be appreciable. Recently, two efficient models have been developed by Shourvarzi and Joodaki [13] and Hu *et al.* [14]. These formulations combine numerical data with a circuit approach. This implies the use of a commercial software for each case of aperture and consequently a waste of time that can be avoided by using an analytical approach. This is one of the reasons our formulation is completely analytical.

Our proposal aims to overcome the restrictions typifying these valuable formulations. In other words, our analytical model can take into account many complex and off-centered aperture shapes, without approximation (in particular, curved aperture shapes in all directions), and simulate the high order resonant modes of the lossy enclosure. In order to attain our objectives, we improved Yin's ILCM to model rigorously, and with a full analytic formula, circular, elliptical, round-ended and cross-shaped apertures, geometrically, as well as electrically. Our formulation is based on Bethe's theory of electrically small apertures. This dictates that the maximal aperture dimension is equal to $1/10$ of the wavelength. Even though this restraint appears rather severe, Bethe's method has proven to be very useful in many applications. Following the study done by Stoneback in [15] we demonstrate the intrinsic impedance of the TL representing the aperture in accordance with the electric and magnetic dipole impedances. This completely new formula lays the foundation for the prediction of SE of enclosures with complex apertures.

The approach proposed in this paper takes into account the effect of high-order waveguide modes and the application of multiple apertures on the basis of a reformulation of the model in [9], described in [16, Sec. II.B]. In Section II, we detail the problematic exposed in this paper, and the equivalent circuit model. The first technique is summarized in Section III for lossy enclosures containing canonical apertures. Section IV focuses on introducing the equivalent dipole impedances in the first formulation as the intrinsic impedance of the aperture. In this last section, the entire development is detailed to reveal the final SE formula. In Section V, the analytical results are validated by using a commercial tool for a range of configurations of perforated enclosures. First, the analysis is focused on a circular aperture in order to validate our formulation. Secondly, the studied configurations contain

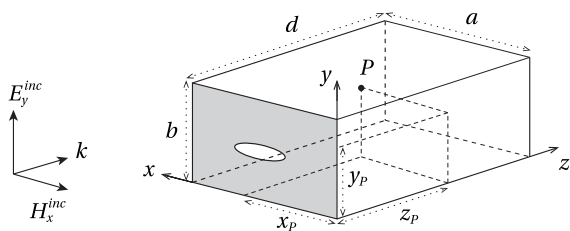


FIGURE 1. Geometry of the problem of a rectangular enclosure containing one or multiple apertures on its front face, illuminated by a plane wave, and the location of the observation point P (x_p, y_p, z_p) for SE evaluation.

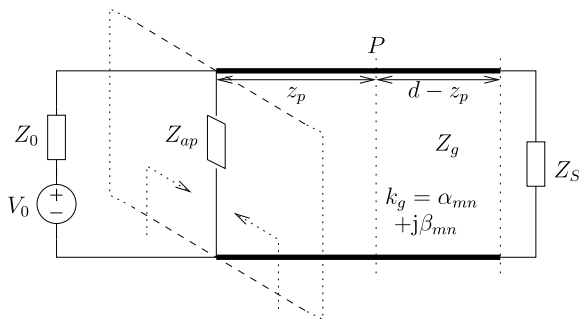


FIGURE 2. Equivalent circuit model.

elliptical apertures. Thirdly, the evaluation concerns complex apertures, such as round-ended and cross-shaped.

II. CIRCUIT MODEL DESCRIPTION

We consider a lossy rectangular enclosure of dimensions $a \times b \times d$ containing one or several apertures illuminated by an external plane wave polarized vertically (\hat{y} direction) travelling in the direction \hat{z} (see Fig.1). As mentioned above, the ILCM formulation gives a simple circuit representation of the problem of an enclosure containing a circular aperture, drawn in Fig.2. The enclosure is taken as a lossy waveguide, represented by a TL. Thus, the waveguide propagation constant is taken as lossy. The TL extremities are modified to take into account the incident plane wave, apertures and wall conductivity. The external radiation is modeled by an equivalent voltage generator V_0 and its internal impedance Z_0 . represents the aperture presence and its influence on the circuit model. The losses due to the conductivity of the back wall are modeled with the surface impedance Z_S . The next section summarizes the mathematical circuit model for canonical apertures. Complete description is available in [17].

III. EM FIELDS IN A LOSSY CAVITY CONTAINING CANONICAL APERTURES

The excitation is represented by V_0 and Z_0 , at $z = 0$, in terms of E_y^{inc} as in [8], evaluated by $V_0 = E_y^{inc} \times \sqrt{ab}$ using the definition of the EM power transmitted through a surface and Poynting’s vector. The impedance Z_0 is the vacuum impedance, equal to $Z_0 = \sqrt{\mu_0/\epsilon_0}$. The aperture impedance Z_{ap}^{tot} , improved by Yin and Du [9] for multiple apertures is given in accordance with Z_{eq} , the equivalent impedance of

the coplanar microstrip line that represents the aperture. For canonical apertures, this equivalent impedance is given by Gupta et al. [18]. However, this formula can only cope with rectangular apertures. Even circular apertures are approximated by square ones of identical surface. The propagation constant of the equivalent TL, representing the waveguide, contains, in this lossy formulation, an attenuation constant that includes losses in longitudinal waveguide walls. For the Transverse Electric (TE) modes, the propagation constant is $k_g^{TE} = \alpha_{mn}^{TE} + j\beta_{mn}$, and, for the Transverse Magnetic (TM) modes, $k_g^{TM} = \alpha_{mn}^{TM} + j\beta_{mn}$. Attenuation constants α_{mn}^{TE} and α_{mn}^{TM} are given in [16]. The waveguide end at $z = d$ is taken, loaded with $Z = Z_S$. This surface impedance Z_S is related to the material conductivity σ as $Z_S = R_S + jX_S = (1 + j)/(\sigma \delta)$, where δ is the skin depth. Finally, for the TE modes, the equivalent voltage V_{eq} on the line representing the lossy waveguide is given by the equation,

$$V_{eq,loss}^{TE}(z_p) = \frac{1 + \Gamma_2 \exp(-2k_g^{TE}d) \exp(2k_g^{TE}z_p)}{1 - \Gamma_1 \Gamma_2 \exp(-2k_g^{TE}d)} \times \frac{Z_g^{TE}}{Z_g^{TE} + Z_1} V_1 \exp(-k_g^{TE}z_p) \quad (1)$$

where $V_1 = V_0 Z_{ap}^{tot} / (Z_0 + Z_{ap}^{tot})$ and $Z_1 = Z_0 Z_{ap}^{tot} / (Z_0 + Z_{ap}^{tot})$ are the voltage and impedance of the equivalent generator representing the plane wave coupled to the aperture, respectively. The parameter $\Gamma_1 = (Z_1 - Z_g^{TE}) / (Z_1 + Z_g^{TE})$ is the reflection coefficient of the line at $z = 0$ and the parameter $\Gamma_2 = (Z_S - Z_g^{TE}) / (Z_S + Z_g^{TE})$ is the reflection coefficient of the line at $z = d$ (the loaded termination). For the TM modes, the equivalent voltage $V_{eq,loss}^{TM}(z_p)$ is also given by (1) replacing $Z_g^{TE} = j\omega\mu/k_g^{TE}$ with $Z_g^{TM} = k_g^{TM} / (j\omega\epsilon)$ and k_g^{TE} with k_g^{TM} . Frequencies are also modified since losses introduce a frequency shift due to quality factor Q_{loss} , as, $f_{loss} = f(1 - 1/(2Q_{loss}))$.

Then, EM fields are given in terms of $V_{eq,loss}$ as in [16], considering the contribution of the TE and TM modes.

IV. MODIFICATION FOR COMPLEX APERTURES

A. APERTURE DIPOLE IMPEDANCE

This paper deals with the inclusion of realistic geometry apertures. Our proposal is a first step in the improvement of ILCM models applied to different shapes of apertures. In particular, we focus here on circular, elliptical, round-ended and cross-shaped apertures for validation. We propose a reformulation of the equivalent impedance of the aperture Z_{eq} on the basis of Bethe’s theory [19]. He demonstrates that the radiative behavior of an aperture, in a perfectly conducting thin sheet, can be represented by equivalent electric and magnetic dipoles. The electric dipole is oriented perpendicular to the aperture, in the direction \hat{z} . Magnetic dipoles are oriented transverse to the aperture plane. Each dipole is defined by a dipolar moment depending on its orientation. These dipole moments are related to the short-circuited field (when the aperture is totally obstructed by a conductive material)

by proportionality coefficients that are only functions of shape and size of the aperture. These coefficients are known as electric and magnetic polarizabilities α_e^P , α_{mx}^P and α_{my}^P . In order to include these coefficients in our ILCM, we rely on [15]. In his article, Stoneback proposed an improvement to Mautz and Harrington’s work [20] wherein the dipole impedances of the apertures are calculated in terms of their polarizabilities on the basis of Bethe’s formulation. In our method, the aperture is not geometrically replaced by these equivalent dipoles, but the analytical formulas of the dipole impedances developed by Stoneback are introduced as the intrinsic impedance of the transmission line representing the aperture. It can be noticed that the far field evaluation restriction is not valuable here since we only consider the polarizability of the apertures established by Bethe in the circuit model. Indeed, those polarizabilities are not field dependent but only depend on the shape and the size of the aperture. The derived dipole impedance formulas depend on the polarizability of the apertures being considered, having been analytically demonstrated under the limitation of small apertures [15].

Hence, for the TE modes, the magnetic dipole impedance along $u = \{x, y\}$ is given by Stoneback in [15] as,

$$Z_{mu}^{TE} = \frac{1}{2} \left(\frac{S (k_g^{TE})^2}{3\pi Z_g^{TE}} + \frac{S}{j\omega\mu_0\alpha_{mu}^P} \right)^{-1} \quad (2)$$

where S represents the aperture surface, Z_g^{TE} and k_g^{TE} are the intrinsic impedance and the propagation constant of the equivalent TL representing the waveguide, respectively. Again, for the TE modes, the electric dipole impedance derived by Stoneback [15] is given by,

$$Z_e^{TE} = 2 \left(\frac{Sb_e^2(k_g^{TE})^4}{3\pi Z_g^{TE}} + \frac{j\epsilon_0\omega S b_e^2}{\alpha_{mu}^P} \right)^{-1} \quad (3)$$

where b_e is, according to Stoneback, interpreted as an effective minimum thickness of the aperture, and equal to $b_e = S/l_e$. The parameter l_e defines the effective electric dipole length as $1/l_e = 1/l_{mx} + 1/l_{my}$, where l_{mu} is the effective magnetic dipole length. According to Stoneback l_{mu} is obtained by integrating the path length of the magnetic currents \hat{M}_{mu} on both sides of the aperture.

$$l_{mu} = 2 \int \int \hat{M}_{mu} \cdot d\hat{l}_{mu} d\theta \quad (4)$$

where \hat{M}_{mu} is taken perpendicular to $\theta = 0$ for $u = \{x, y\}$. For the TM modes, the expressions of Z_{mu} and Z_e are also valuable by replacing Z_g^{TE} with Z_g^{TM} and k_g^{TE} with k_g^{TM} .

Each dipole impedance is then defined by its magnetic polarizability along x and y , α_{mx}^P and α_{my}^P , its electric polarizability, α_e^P , its surface S and the length of the electric dipole l_e . Those five parameters are detailed for each aperture studied, as shown in 1. A schematic representation of these apertures

is also given in Table 1. In this paper, four shapes of apertures are analyzed: circular, elliptical, round-ended and cross-shaped. Analytical expressions of the magnetic and electric polarizability have been computed for circular apertures by Bethe in [19]. For elliptical apertures, analytical expressions are given by Taylor in [21]. They are expressed in terms of $K(e^2)$ and $E(e^2)$, the complete elliptic integrals of the first and second kind. These integrals are given by,

$$K(e^2) = \int_0^{\pi/2} \frac{d\phi}{\sqrt{1 - e^2 \sin^2 \phi}} \quad (5)$$

$$E(e^2) = \int_0^{\pi/2} \sqrt{1 - e^2 \sin^2 \phi} d\phi \quad (6)$$

where e represents the aperture eccentricity, $e = \sqrt{1 - (r_2/r_1)^2}$. When $e = 0$, the aperture is circular. When $0 \leq e \leq 1$, the aperture is elliptical.

For round-ended apertures and cross-shaped apertures, there is no analytical formula. However, Macdonald proposed polynomial approximations for round-ended apertures in [25]. Electric polarizability of this type of aperture is in accordance with the 4th degree polynomial $h_e^R(w/l)$, given by,

$$h_e^R\left(\frac{w}{l}\right) = \frac{\pi}{16} \left(\frac{w}{l}\right)^2 \left[1 - 0,7650\frac{w}{l} + 0,1894\left(\frac{w}{l}\right)^2 \right] \quad (7)$$

In his paper, Macdonald compared his formulation to the experimental data obtained by Cohn in [26] and obtained a relative error lower than 1%. Thus, his approximation has been validated for round-ended apertures. Two other articles, also published by Macdonald, give the magnetic polarizability of the round-ended aperture, along x in [22], and along y in [24]. The 3rd degree polynomial are given by the following formulas,

$$f_{mx}^R\left(\frac{w}{l}\right) = \frac{0,187 + 0,052\left(\frac{w}{l}\right)\left(1 - \frac{w}{l}\right)}{\ln\left(1 + 2,12\frac{l}{w}\right)} \quad (8)$$

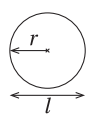
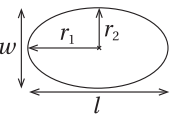
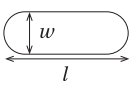
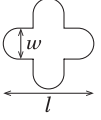
$$g_{my}^R\left(\frac{w}{l}\right) = \frac{\pi}{16} \left(\frac{w}{l}\right)^2 \left[1 - 0,512\left(\frac{w}{l}\right) \right] \quad (9)$$

The magnetic polarizability along x determined by Macdonald shows a relative error of 1.4% against the numerical solution given by De Smedt and Van Bladel in [27], and 1.7% against Cohn’s measurements given in [23]. Along y , the polynomial approximation of the magnetic polarizability developed by Macdonald shows a relative error of 1.8% against Cohn’s measurements. Concerning cross-shaped apertures, the electric and magnetic polarizabilities are given by Cohn’s experimental results in [26] and [23].

B. TOTAL APERTURE IMPEDANCE

Three dipole impedances define each aperture for both the TE and the TM modes. We consider that each magnetic dipole has a different interaction with the electric one. The combination of dipoles gives a power assessment equal to

TABLE 1. Configurations of studied cases using a lossy enclosure of dimensions 30 × 12 × 26 cm of electrical conductivity $\sigma = 10^5$ S/m containing complex apertures.

Aperture	Circular	Elliptical	Rounded end slot	Cross
Shape				
Magnetic Polarizability along x α_{mx} (C.m ² .V ⁻¹)	calculated by Bethe [19] $\frac{4}{3}r^3$	calculated by Taylor [21] $\frac{\pi}{3} \frac{r_1^3 e^2}{K(e^2) - E(e^2)}$	McDonald polynomial [22] $l^3 f_{mx}^R \left(\frac{w}{l}\right)$	measured by Cohn [23]
Magnetic Polarzability along y α_{my} (C.m ² .V ⁻¹)	calculated by Bethe [19] $\frac{4}{3}r^3$	calculated by Taylor [21] $\frac{\pi}{3} \frac{r_1^3 e^2 (1 - e^2)}{E(e^2) - (1 - e^2)K(e^2)}$	McDonald polynomial [24] $l^3 g_{my}^R \left(\frac{w}{l}\right)$	measured by Cohn [23]
Electric Polarizability α_e (C.m ² .V ⁻¹)	calculated by Bethe [19] $-\frac{2}{3}r^3$	calculated by Taylor [21] $-\frac{\pi}{3} \frac{r_1^3 (1 - e^2)}{E(e^2)}$	McDonald polynomial [25] $l^3 h_e^R \left(\frac{w}{l}\right)$	measured by Cohn [26]
Surface S (m ²)	πr^2	$\pi r_1 r_2$	$\pi \left(\frac{w}{2}\right)^2 + w \times (l - w)$	$2wl + \left(\frac{\pi}{2} - 3\right) w^2$
Electric dipôle length l_e (m)	$4r$	$2\sqrt{2(r_1^2 + r_2^2)}$	$4w$	$\frac{w}{2}(16 - \pi)$

$P = P_e + P_m$, where P_e is the power delivered by the electric dipole, and P_m represents, indiscriminately, the power delivered by the magnetic dipole along x , P_{mx} , or the power delivered by the magnetic dipole along y , P_{my} . Then, $P = 1/2|V_e|^2 Y_e + 1/2|V_{mu}|^2 Y_{mu}$, where Y_e and Y_{mu} are the equivalent admittances of electric and magnetic (along $u = x, y$) dipoles. In his article, Stoneback makes the assumption [15] that voltage $|V_e|$ and $|V_{mu}|$ have the same magnitude. Consequently, $|V_e| = |V_{mu}| = |V|$, and $P = 1/2|V|^2(Y_e + Y_{mu})$. According to this relation and Stoneback’s assumption, the electric and magnetic dipole admittance are arranged in series. This implies that the equivalent dipole impedance must be parallelly arranged in the final circuit. Since the radiation of the magnetic dipole is defined by two impedances, one along x , one along y , we can define two equivalent impedances, one corresponding to the magnetic dipole along x with the electric dipole, and one corresponding to the magnetic dipole along y with the electric dipole. Those equivalent impedances are given by,

$$Z_{eq,u} = Z_{mu} || Z_e = \frac{Z_{mu} Z_e}{Z_{mu} + Z_e} \quad (10)$$

This formulation relates back to the first formulation of Robinson, and the improvement developed by Yin. Indeed, the aperture is modeled by a short-circuited transmission line. However, the intrinsic impedance of the TL is replaced by the equivalent impedance that describes the curves of the aperture as per Stoneback’s approach. The aperture impedance depends not only on this modified equivalent intrinsic impedance but also on the TL length l and its behavior. According to Yin, and to our formulation, the total aperture impedance is defined for each orientation $u = \{x, y\}$, as,

$$Z_{ap,u}^{tot} = \sum_{i=1}^{N_{ap}} \frac{l_i}{2a} j Z_{eq,u} \tan \frac{\beta l_i}{2} \times \sin \frac{m\pi x_{c,i}}{a} \cos \frac{n\pi y_{c,i}}{b} \quad (11)$$

Since the ILCM presented here can cope N_{ap} apertures, each aperture is enumerated in this previous expression by the indice i . The aperture i of length l_i is defined by its center $(x_{c,i}, y_{c,i})$.

C. FINAL CIRCUIT MODEL

Since the aperture behavior is modeled by a TL of intrinsic impedance $Z_{eq,u}$, when considering both of the magnetic dipoles $u = \{x, y\}$, the final circuit model is divided into two sub-circuits. One considering the interaction between the electric dipole and the magnetic dipole along x , and the other one considering the interaction between the electric dipole and the magnetic dipole along y . The calculation process is defined as follows.

- 1) The equivalent intrinsic impedance $Z_{eq,u}$ is calculated along both orientations $u = \{x, y\}$. Then, the total aperture impedance $Z_{ap,u}^{tot} = f(Z_{eq,u})$ obtained, is given by (11).
- 2) The two sub-circuits provide the equivalent voltages at $z = z_p$, designated by $V_{eq,loss,x}(z_p)$ and $V_{eq,loss,y}(z_p)$ given by the equation (1) in Section III, for the TE and TM modes.
- 3) The equations for the total electric field, considering the contribution of the TE and TM modes, are given by the formulas in [16], in Section II.B, for both sub-circuits. The interaction of the magnetic dipole, along x , with the electric dipole gives, $E_{h,x}^{tot} = E_{h,x}^{TE} + E_{h,x}^{TM}$, where E_h designates E_x, E_y or E_z arbitrarily. The interaction of the magnetic dipole, along y , with the electric dipole gives, $E_{h,y}^{tot} = E_{h,y}^{TE} + E_{h,y}^{TM}$.
- 4) The contribution of each of the interactions between both dipoles, that is represented by the contribution of both sub-circuits, $E_{h,x}^{tot}$ and $E_{h,y}^{tot}$ is combined to obtain the total electric field E_h^{tot} . In fact, E_h^{tot} is the h-component of the field vector $\mathbf{E}_h^{tot} = E_{h,x}^{tot} \mathbf{u}_x + E_{h,y}^{tot} \mathbf{u}_y$.

5) The total electric field vector is given by,

$$\mathbf{E}^{\text{tot}} = E_x^{\text{tot}}\mathbf{u}_x + E_y^{\text{tot}}\mathbf{u}_y + E_z^{\text{tot}}\mathbf{u}_z \quad (12)$$

By definition, the shielding effectiveness of an enclosure is equal to the ratio of the magnitude of the transmitted electric field, represented by E^{tot} to the magnitude of the incident electric field. Finally, the shielding effectiveness of the perforated enclosure is calculated with the formula,

$$SE_{\text{dB}} = -20 \times \log \frac{\sqrt{|E_x^{\text{tot}}|^2 + |E_y^{\text{tot}}|^2 + |E_z^{\text{tot}}|^2}}{E_{\text{inc}}^{\text{tot}}} \quad (13)$$

where $E_{\text{inc}}^{\text{tot}}$ is the magnitude of the total incident electric field.

V. NUMERICAL VALIDATION

This last section is dedicated to the numerical validation of the ILCM developed in this paper. The SE predictions generated by the ILCM proposed here are compared to those obtained from numerical modeling. The commercial software CST Studio Suite[®] (Microwave studio module, Finite Integration Technique Time-domain (TD) solver), is considered as the reference. The SE is evaluated across a frequency range of 0.5 - 2.5 GHz. All the modes up to $m = 5$ and $n = 5$ are considered in order to ensure that all the propagating modes below 2.5 GHz are included in this formulation. For each case studied here, the enclosures have the same dimensions ($30 \times 12 \times 26$ cm) and thickness ($t = 1$ mm), and is taken as lossy. Wall conductivity is chosen equal to $\sigma = 10^5$ S/m, which satisfies the good conductor assumption $\sigma \gg \epsilon_0\omega$. It can be noticed that the front face of the enclosure is taken as PEC since losses due to the aperture are significantly higher than losses due to wall material. The perforated enclosure is excited by a normal incident plane wave polarized in the direction y with a magnitude of $E_{\text{inc}}^{\text{tot}} = 10$ V/m and traveling in the direction z .

For validation, the analysis is divided into three steps. The first one is dedicated to a centered, circular aperture. The results obtained with the ILCM proposed here are compared to numerical results but also to the results obtained using the earlier formulation of the ILCM, where the circular aperture is modeled by a square one that has the same surface, as in [17]. The second step considers three different types of enclosures containing elliptical apertures. Finally, the third and last step focuses on round-ended apertures and cross-shaped apertures.

A. CIRCULAR APERTURE

In order to validate our formulation, the first analysis, named case C1, focused on a centered, circular aperture (radius = 1.3 cm). The results given by our ILCM are compared to the ILCM developed in [17]. Both models are also compared to the numerical results obtained using the commercial software CST Studio Suite[®] in Fig.3. The observation point is located at $P(15, 6, 17.5)$ cm.

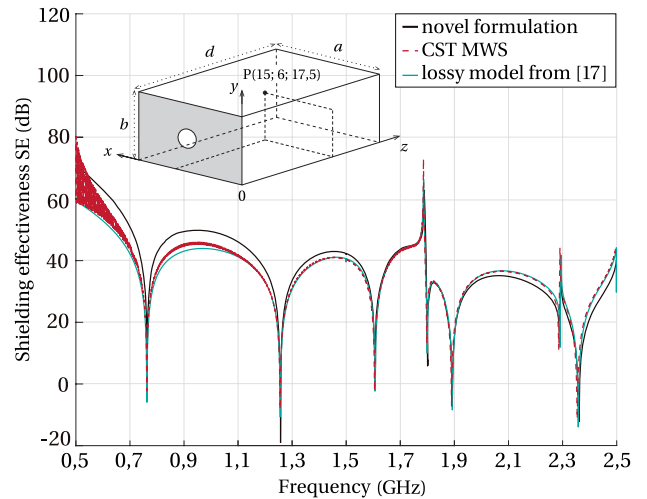


FIGURE 3. Comparison of the SE (case C1) predicted by the model and calculated with CST Studio Suite[®] at point $P(15, 6, 17.5)$ cm and the formulation of model in [17] for an enclosure containing a centered, circular hole.

The SE calculated by these models reveals that both of them present a very good agreement with the SE prediction of the commercial software. The average difference between CST Studio Suite[®] and our ILCM on the frequency range 0.5-2.5 GHz is equal 3.3854 dB. All results in this paper are presented between 0.5 GHz and 2.5 GHz. However, our frequency range of interest is limited to 0.7GHz-2GHz. Indeed we start the analysis from the first resonant frequency up to high frequencies, where many excited modes, and consequently many interactions, make the SE unstable. The purpose of this unusual very large frequency range for this kind of study is to show the limitations of the different models. We have used the Feature Selective Validation (FSV) methodologies that are embodied in IEEE Standard 1597.1 [28], [29] for the comparison of results. The FSV method gives a classification of a point by point difference calculation into 6 categories, Excellent, Very Good, Good, Fair, Poor, and Very Poor. For the case C1, a magnitude agreement of 96.91% was found for the first three categories of the FSV tools. In our formulation, the aperture polarizabilities, α_e^P and α_{mu}^P are constants on the entire range of frequencies. Wen-Hao Cheng demonstrates in [30] that polarizability is frequency dependent. He developed an analytical solution for circular holes in an infinite screen. He expresses the aperture polarizability for the TM_{0nl} modes and the aperture susceptibility for the TE_{1nl} and TM_{1nl} modes. However, this formulation ignores some resonant modes. In this regard, in order to include this approach in our formulation, we would have to improve the formula to include all resonant modes. As well, Stoneback also assumed that the considered aperture is cut in an infinite screen, whereas here, the enclosure wall containing the aperture has finite dimensions. The plane boundaries might cause some errors in the analytical formulation since their impact is not taken into account in Stoneback's formula, nor in Cheng's development for polarizability dependence.

TABLE 2. Configurations of studied cases using a lossy enclosure of dimensions 30 × 12 × 26 cm of electrical conductivity $\sigma = 10^5$ S/m containing complex apertures.

CASE (related figure)	Aperture(s) Dimensions and Positions	Aperture center (x_c, y_c)	Observation Point $P(x_P, y_P, z_P)$
C2 (Fig. 4)	centered $r_1 = 2.2$ cm et $r_2 = 0.7$ cm	(15, 6)	$P(24.5, 8.5, 21.5)$
C3 (Fig. 5)	off-centered $r_1 = 2.2$ cm et $r_2 = 0.7$ cm	(8.5, 4.5)	$P(24.5, 8.5, 21.5)$
C4 (Fig. 6)	staggered array of seven holes $r_1 = 2.2$ cm et $r_2 = 0.7$ cm	Aperture (1) (9, 6)	$P(15, 6, 5.5)$

Consequently, we have not included this frequency dependence since there is no guarantee that it would improve our ILCM technique. Our formulation does present, however, a significant advantage. The real geometry of the aperture is taken into account in our formulation by means of aperture polarizability. This ILCM is able to model enclosures that contain aperture shapes that have not been addressed analytically up to now. Elliptical apertures are usually employed to represent singular apertures of regular shape since the equivalent elliptical aperture is defined with the same surface and the same eccentricity. Consequently, the following application of our ILCM focuses on enclosures containing elliptical apertures.

B. COMPLEX APERTURES

1) ELLIPTICAL APERTURES

To the best of our knowledge, the only analytical technique developed for elliptical apertures has been proposed by Hong Yi et al. [10]. The aperture is represented by short TLs, connected in series, to model the aperture curves. However, since its formulation is based on Robinson’s ILCM, their approach is restricted to the TE_{10p} resonant modes. Thus, a comparison with this formulation would involve improving its formulation to high-order modes for a correct comparison. In this paragraph, the results obtained using our formulation are only compared to numerical results. For validation, three cases are considered, shown in Table 2. The case C2 (see Table 2) considers a single, centered elliptical aperture. The SE calculated with our proposed ILCM is compared to the SE predicted by CST Studio Suite® on Fig. 4. On the same graph, we include the results obtained by CST for a circular aperture that has the exact same surface. In the second case, the same single elliptical aperture is taken off-centered. For both cases the observation point is located at $P(24.5, 8.5, 21.5)$ cm. Thus, on Fig. 5(a), the results predicted with the ILCM developed here and CST Studio Suite® are compared to the results given for the ILCM in Fig. 4, in order to analyze the impact of the aperture position. The case C4 focuses on a staggered array of elliptical apertures that represent a ventilation panel. Results are shown in Fig. 6.

For all of the configurations, the SE calculated with our ILCM are in good agreement with the commercial software

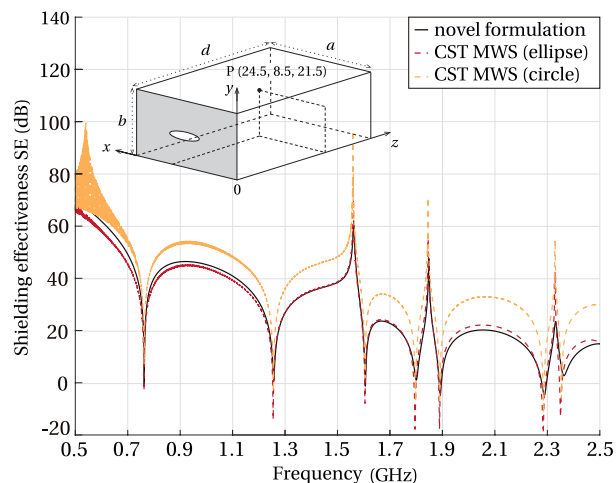
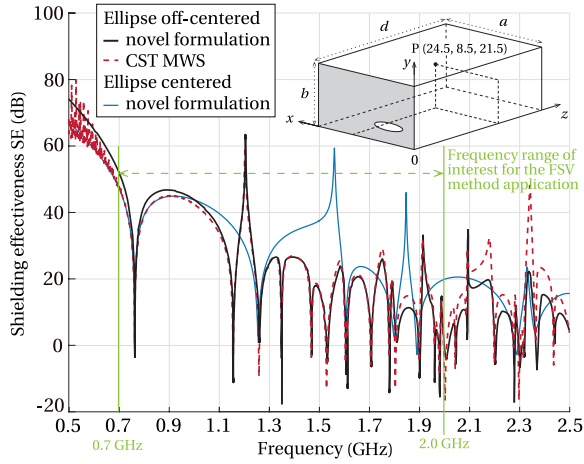
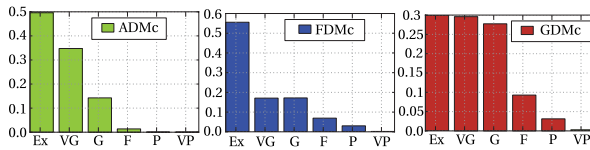


FIGURE 4. Comparison of the SE (case C2, Table 2), predicted by the model and calculated with CST Studio Suite® at point $P(24.5, 8.5, 21.5)$ cm for an enclosure containing a centered elliptical hole.

CST Studio Suite®. Naturally, resonances of the perforated enclosure being considered are correctly predicted throughout the entire range of frequencies. Regarding case C2, the SE predicted by CST Studio Suite®, for a single, centered, elliptical aperture and the SE predicted also by CST Studio Suite®, for a single, circular aperture are significantly different in magnitude. Even though the aperture surface is exactly the same, the aperture shape clearly has an influence on the SE of the perforated enclosure. For a circular aperture, the SE is higher by approximately 10 dB. Concerning case C3, the only difference between it and case C2 is the aperture position on the front face of the enclosure that is located consciously in the vicinity of the corner of the enclosure. It can be noticed that the enclosure response is totally different. The off-centered aperture excites more modes than the centered aperture. The coupling between the incident plane wave and the front face of the enclosure, containing the aperture, is not the same in both cases, despite the fact that the apertures are exactly the same. When specifically considering the SE predicted for the off-centered aperture, magnitude errors appears only above 2 GHz. There is some discrepancies that might be caused by the frequency dependance of polarizabilities. As the circular case, the FSV method is applied to the range of frequencies of interest between 0.7 GHz and 2.0 GHz. In Fig. 5(b) the ADM, FDM and GDM histograms are given. The magnitude ADM histogram gives a categories distribution more significant in the first three categories, Excellent, Very Good and Good. The percentage of agreement between the model presented and the numerical solver CST studio suite is equal in the Excellent category of 49.61%. In the Very Good category and the Good category, the FSV results for the ADM comparison are equal to 34.77% and 14.26%, respectively. Regarding the FDM and the GDM histogram, most of the results have fallen into the first three categories. The FDM histogram shows 89.85% of agreement and the GDM histogram shows 87.30% of agreement. These results are very encouraging considering that the aperture



(a) SE comparison calculated by the model and CST studio suite®



(b) Results from FSV IEEE method on 0.7-2.0 GHz

FIGURE 5. Comparison of the SE (case C3, Table 2), predicted by the model and calculated with CST Studio Suite® at point P(24.5, 8.5, 21.5) cm for an enclosure containing an off-centered elliptical hole and FSV histograms ADM, FDM and GDM calculated with the FSV IEEE method on the frequency range 0.7-2.0 GHz.

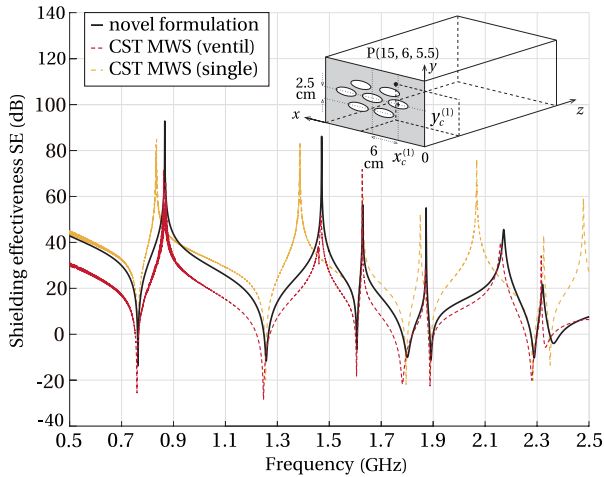


FIGURE 6. Comparison of the SE (case C4, Table 2), predicted by the model and calculated with CST Studio Suite® at point P(15, 6.5, 5.5) cm for an enclosure containing a ventilation of elliptical apertures.

is located in the vicinity of the front panel of enclosure. The aperture impedance developed by Stoneback is given for an aperture on a sheet of metal. But, in our formulation, the dimensions of the front panel and the location of the aperture are also included in the process. These are combined in the circuit model to create an intermediate source that represent the incident plane wave coupled with the aperture in a finite screen (the front panel). On this frequency range of interest the mean of the point by point magnitude difference calculation is 2.2833 dB. On the entire frequency range this mean is equal to 3.7459 dB. These average differences are

TABLE 3. Configurations of studied cases using a lossy enclosure of dimensions 30 × 12 × 26 cm of electrical conductivity $\sigma = 10^5$ S/m containing complex apertures.

CASE (related figure)	Aperture(s) Dimensions and shape	Aperture center (x_c, y_c)	Observation Point $P(x_P, y_P, z_P)$
C5 (Fig. 7)	rounded-end centered $l = 3.7$ cm et $w = 1.6$ cm	(15, 6)	$P(22, 10.5, 21.5)$ $P(15, 6, 6)$
C6 (Fig. 8)	cross centered $l = 3.6$ cm $w = 0.9$ cm	(15,6)	$P(22, 10.5, 4)$ $P(4.75, 4.75, 6.5)$

completely acceptable since it is an analytical prediction model. This leads to the conclusion that despite the approximations involved concerning the vicinity of the aperture and the corner of the front panel, the formulation presented in this paper could be very useful for SE prediction. Case C4, gives a SE prediction at an observation point close to the aperture in order to prove that the restriction to the far field, from Bethe’s theory, has been excluded from the formulation. Since we have been relying on Stoneback’s formulation in [15], we made the assumption that the model includes an electric representation of the aperture behavior through its polarizabilities, and, of course, its geometrical description. Considering that the results obtained are in good agreement with CST Studio Suite®, we can conclude that our model is correct. However, we observe, in this case, a magnitude error that decreases on the frequency bandwidth. The neglected frequency dependence of the polarizabilities has more influence in this case since there are more apertures. On the same graph, we have graphed the SE predicted by CST Studio Suite® at the same observation point as for the case of the centered, elliptical aperture. Both aperture configurations (single, centered, and ventilation) scatter the incident plane wave in different manners and, consequently, excite different resonant modes.

Regarding all of the results in this paragraph, the impact of the aperture is correctly taken into account, and, it can be seen that our model is reliable, accurate and fast for SE prediction of enclosures containing elliptical apertures.

2) OTHER APERTURES FORMS

This last part is dedicated to complex apertures with curved edges. These apertures have never been included in an ILCM representation of a perforated enclosure before. Two configurations are exposed. Case C5 considers, a centered, round-ended aperture and case C6, a centered, cross-shaped aperture. For both configurations, the SE predictions are given at two observation points. All case details are presented in Table 3.

For all configurations, the SE predicted by the model and the commercial software CST Studio Suite® are in good agreement in terms of the description of the behavior of the enclosure. As in the previous cases, a magnitude error is observed. This gap might be caused by the frequency dependence and is neglected in our formulation, but also by the approximations used to calculate the polarizabilities of the apertures. Indeed, for round-ended apertures, the

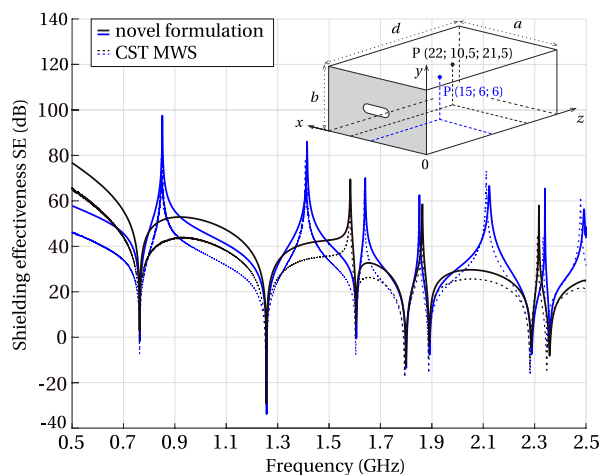


FIGURE 7. Comparison of the SE (case C5, Table 3), predicted by the model and calculated with CST Studio Suite® at two observation points for an enclosure containing a centered round-ended aperture.

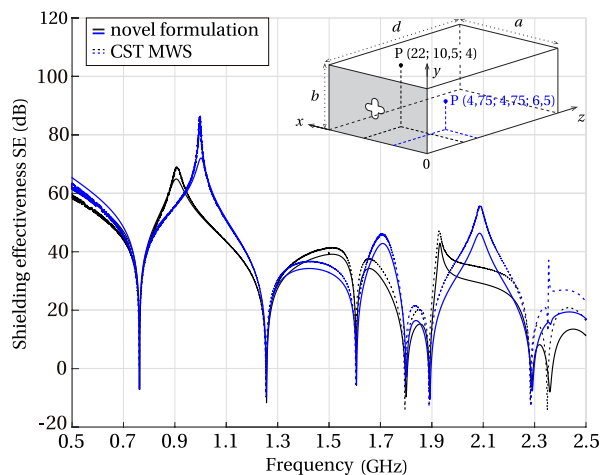


FIGURE 8. Comparison of the SE (case C6, Table 3), predicted by the model and calculated with CST Studio Suite® at two observation points for an enclosure containing a centered cross hole.

polarizabilities are given by polynomial approximations. For cross-shaped apertures, the polarizabilities are given by measurements. For circular and elliptical apertures, the formulation relies on the analytical expressions of α_{mu}^P and α_e^P giving them a more rigorous evaluation of the aperture impedances. The results obtained with the ILCM presented here are very encouraging as they are very similar to the results given by CST Studio Suite® evaluations in terms of tendencies. This is especially true for the SE prediction of the enclosures that contain complex apertures, such as round-ended or cross-shaped ones; the latter never having been included in previous analytical work to our knowledge. As mentioned above, one of the most relevant advantages of the analytical formulation that we are presenting is the speed of the simulation. It takes less than 2 seconds to reach an appreciable evaluation.

VI. CONCLUSION

In this paper, we have focused on a full analytical approach to evaluate the shielding effectiveness of metallic shields that

contain complex aperture shapes. The approach is based on Yin’s reliable circuit model, where the enclosure and the aperture are modeled as transmission lines. Our formulation combines this existing model with Bethe’s theory of diffraction by small holes and including Stoneback’s equivalent dipole impedances. We replaced the initial intrinsic impedance by Stoneback’s equivalent dipole impedances, given in terms of aperture polarizability. The formulation takes into account the electric behavior of the aperture and its geometrical representation. In this paper, our objective was not to develop another aperture model but a global model that includes the aperture and the enclosure behavior. Each model we used is certainly well-known but, their combination, in this context, considering the limitations of Bethe theory that we have been able to overcome, is new. Thus being, the analytical approach developed can cope with four different aperture shapes, such as cross-shaped apertures and round-ended apertures, which have never previously been included in ILCM computation, to the best of our knowledge. In this paper, different configurations have been computed with our ILCM for enclosures containing circular, elliptical, round-ended and cross-shaped apertures. The analytical formulation presented in this paper provides results in good agreement with the commercial software CST Studio Suite®. The focus of our ILCM technique was not to compete with existing approaches. Our aim was to develop a model capable of dealing with different aperture shapes to provide a helpful tool for engineers in predicting the SE of shielding devices. The presented analytical formulation gives a good SE evaluation in less than two seconds, compared to hours with a rigorous numerical solver. This major advantage, combined with the reliability of the formulation, makes the proposed solution significant for intensive simulations (optimization, stochastic or parametric studies). The analytical formulation relies on Bethe’s theory and, thus, presents the same restriction to electrically small apertures, which are the most widespread size. Electrically small apertures are used for ventilation panels or control panels, for example. The approach presented in this paper constitutes a starting point to complex aperture modeling in SE analytical techniques. In future work, we would enhance the accuracy of the model for round-ended and cross-shaped apertures, but also extend the formulation to loaded apertures sealed by conducting gaskets, large apertures and thin apertures, such as slots.

REFERENCES

- [1] A. F. Peterson, S. L. Ray, R. Mittray, *Computational Methods for Electromagnetics*, Piscataway, NJ, USA: IEEE Press, 1998.
- [2] W. C. Chew, J. M. Jin, E. Michielssen, and J. M. Song, *Fast and Efficient Algorithms in Computational Electromagnetics*, Norwood, MA, USA: Artech House, 2001.
- [3] A. Taflove and S. C. Hagness, *Computational Electrodynamics: The Finite-Difference Time-Domain Method in Computational Electrodynamics II*, vol. 3, 2nd ed. Norwood, MA, USA: Artech House, 1996.
- [4] M. N. O. Sadiku, *Numerical Techniques in Electromagnetics*, 2nd ed. Boca Raton, FL, USA: CRC Press, 2000.
- [5] S. Celozzi, R. Araneo, and G. Lovat, “Numerical methods for shielding analyses,” in *Electromagnetic Shielding*, Hoboken, NJ, USA: Wiley, 2008, ch. 5, pp. 87–143.

- [6] M. P. Robinson, T. M. Benson, C. Christopoulos, J. F. Dawson, M. D. Ganley, A. C. Marvin, S. J. Porter, and D. W. P. Thomas, "Analytical formulation for the shielding effectiveness of enclosures with apertures," *IEEE Trans. Electromagn. Compat.*, vol. 40, no. 3, pp. 240–248, Aug. 1998.
- [7] R. Azaro, S. Caorsi, M. Donelli, and G. L. Gragnani, "Evaluation of the effects of an external incident electromagnetic wave on metallic enclosures with rectangular apertures," *Microw. Opt. Technol. Lett.*, vol. 28, no. 5, pp. 289–293, Mar. 2001.
- [8] T. Konefal, J. F. Dawson, A. C. Marvin, M. P. Robinson, and S. J. Porter, "A fast multiple mode intermediate level circuit model for the prediction of shielding effectiveness of a rectangular box containing a rectangular aperture," *IEEE Trans. Electromagn. Compat.*, vol. 47, no. 4, pp. 678–691, Nov. 2005.
- [9] M. C. Yin and P. A. Du, "An improved circuit model for the prediction of the shielding effectiveness and resonances of an enclosure with apertures," *IEEE Trans. Electromagn. Compat.*, vol. 58, no. 2, pp. 448–456, Apr. 2016.
- [10] L. H. Yi, D. Su, C. Yao, and Z. Z. Hua, "Analytically calculate shielding effectiveness of enclosure with horizontal curved edges aperture," *Electron. Lett.*, vol. 53, no. 25, pp. 1638–1640, Dec. 2017.
- [11] J. R. Solin, "Formula for the field excited in a rectangular cavity with an aperture and lossy walls," *IEEE Trans. Electromagn. Compat.*, vol. 57, no. 2, pp. 203–209, Apr. 2015.
- [12] C. R. Collin, *Field Theory of Guided Waves*, 2nd. ed. Hoboken, NJ, USA: Wiley, 1991.
- [13] A. Shourvarzi and M. Joodaki, "Shielding effectiveness estimation of an enclosure with an arbitrary shape aperture," in *Proc. Int. Symp. Electromagn. Compat.*, 2017, pp. 1–4.
- [14] P. Hu, X. Sun, and J. Chen, "Hybrid model for estimating the shielding effectiveness of metallic enclosures with arbitrary apertures," *IET Sci., Meas. Technol.*, vol. 14, no. 4, pp. 462–470, Jun. 2020.
- [15] R. A. Stoneback, "The dipole impedance of an aperture," *Prog. Electromagn. Res. B*, vol. 26, pp. 401–423, 2010.
- [16] A. Rabat, P. Bonnet, K. El Khamlichi Drissi, and S. Girard, "Analytical models for electromagnetic coupling of an open metallic shield containing a loaded wire," *IEEE Trans. Electromagn. Compat.*, vol. 59, no. 5, pp. 1634–1637, Oct. 2017.
- [17] A. Rabat, P. Bonnet, K. E. K. Drissi, and S. Girard, "Analytical formulation for shielding effectiveness of a lossy enclosure containing apertures," *IEEE Trans. Electromagn. Compat.*, vol. 60, no. 5, pp. 1384–1392, Oct. 2018.
- [18] K. C. Gupta, R. Garg, I. Bahl, and P. Bhartia, "Coplanar lines: Coplanar waveguide and coplanar strips," in *Microstrip Lines Slotlines*, 2nd. ed. Norwood, MA, USA: Artech House, 1996, ch. 7, pp. 347–432.
- [19] H. A. Bethe, "Theory of diffraction by small holes," *Phys. Rev. Lett.*, vol. 66, nos. 7–8, pp. 163–182, Oct. 1944.
- [20] J. R. Mautz and R. F. Harrington, "An admittance solution for electromagnetic coupling through a small aperture," *Appl. Sci. Res.*, vol. 40, no. 1, pp. 39–69, 1983.
- [21] C. Taylor, "Electromagnetic pulse penetration through small apertures," *IEEE Trans. Electromagn. Compat.*, vol. EMC-15, no. 1, pp. 17–26, Feb. 1973.
- [22] N. A. McDonald, "Simple approximations for the longitudinal magnetic polarizabilities of some small apertures," *IEEE Trans. Microw. Theory Techn.*, vol. MTT-36, no. 7, pp. 1141–1144, Jul. 1988.
- [23] S. B. Cohn, "Determination of aperture parameters by electrolytic-tank measurements," *Proc. IRE*, vol. 39, no. 11, pp. 1416–1421, Nov. 1951.
- [24] N. A. McDonald, "Polynomial approximations for the transverse magnetic polarizabilities of some small apertures," *IEEE Trans. Microw. Theory Techn.*, vol. MTT-35, no. 1, pp. 20–23, Jan. 1987.
- [25] N. A. McDonald, "Polynomial approximations for the electric polarizabilities of some small apertures," *IEEE Trans. Microw. Theory Techn.*, vol. MTT-33, no. 11, pp. 1146–1149, Nov. 1985.
- [26] S. B. Cohn, "The electric polarizability of apertures of arbitrary shape," *Proc. IRE*, vol. 40, no. 9, pp. 1069–1071, Sep. 1952.
- [27] R. De Smedt and J. Van Bladel, "Magnetic polarizability of some small apertures," *IEEE Trans. Antennas Propag.*, vol. AP-28, no. 5, pp. 703–707, Sep. 1980.
- [28] *IEEE Standard for Validation of Computational Electromagnetics Computer Modeling and Simulations*, Standard 1597.1, 2008, pp. 1–41.
- [29] A. P. Duffy, A. J. Martin, A. Orlandi, G. Antonini, T. M. Benson, and M. S. Woolfson, "Feature selective validation (FSV) for validation of computational electromagnetics (CEM). Part I-the FSV method," *IEEE Trans. Electromagn. Compat.*, vol. 48, no. 3, pp. 449–459, Aug. 2006.
- [30] W.-H. Cheng, A. V. Fedotov, and R. L. Gluckstern, "Frequency dependence of the polarizability and susceptibility of a circular hole in a thick conducting wall," in *Proc. Part. Accel. Conf.*, Dallas, TX, USA, 1995, pp. 3266–3268.



AMÉLIE RABAT received the master's degree in electromagnetic compatibility from Blaise Pascal University, Clermont-Ferrand, France, in 2015, and the Ph.D. degree in EMC from the Institut Pascal, Clermont Auvergne University, in 2019.

Her research interests include electromagnetic shielding, electromagnetic interference problem, and numerical/computational modeling for EMC applications.



PIERRE BONNET received the Engineering degree in physics and the M.Sc. degree from Polytech Clermont, in 1994 and 1994, respectively, and the Ph.D. degree in electromagnetism from Blaise Pascal University, Clermont-Ferrand, France, in 1998.

From 1999 to 2008, he was an Assistant Professor with the Department of Physics and the Institut Pascal, Blaise Pascal University, where he is currently a Full Professor and the Head of the

ElectroMagnetic Compatibility Group. His research interests include in the area of numerical electromagnetic, with an emphasis on electromagnetic compatibility/electromagnetic interference problems, reverberating electromagnetic environment, time reversal, source identification, and stochastic modeling.



KHALIL EL KHAMLICH DRISSI (Senior Member, IEEE) received the Diploma degree in electrical engineering and the M.Sc. degree from École Centrale de Lille, in 1987 and 1987, respectively, and the Ph.D. degree from the University of Lille, in 1990.

He joined Polytech Clermont, in 1990, as an Associate Professor and became a Full Professor, in 2005. He was the Dean of the Electrical Engineering Department, from 2007 to 2011. He was

the Vice President of Research and Innovation, from 2012 to 2016. Currently, he is a Vice Regional Academic Delegate of Research and Innovation (DRARI) for the Auvergne-Rhone-Alpes Region. He was appointed to the rank of knight in the order of academic palms, in 2020. He is an Expert for different French agencies (ANRT, ANR, HCERES, and DGRI). He is the Project Leader and is also responsible for several international projects related to EMC (FP7 Marie Curie, Econet, Cogito, Integram, Cedre, Toubkal, and Tassili). He currently has an on-going collaboration with different companies, such as Vedecom, IFPEN, EDF, France Telecom, and Landis+Gyr. He is currently a Full Professor at the University Clermont Auvergne. He authored or coauthored more than 270 scientific papers published in peer-reviewed journals, presented at international conferences and is an author of six WO patents. His research interests include EMC in power electronics and power systems, in particular numerical modeling, EMI reduction, and converter control. He is currently a Senior Member of IEEE Electromagnetic Compatibility and IEEE Power Electronics societies, since 2018.



SÉBASTIEN GIRARD received the Bachelor of Science degree in applied physics from Nottingham Trent University, in 2001, and the Master of Science degree in electromagnetic compatibility, in 2002.

He is currently a Research Engineer in electromagnetic compatibility with the Institut Pascal's Laboratory. He is also in charge of the Electromagnetic Compatibility Laboratory. His research interests include reverberation chamber,

shielding effectiveness, cable harnesses, multi-physics (especially bio-EM), and time/frequency domain measurements in EMC.

...